A Recurrent Missense Mutation in *ZP3* Causes Empty Follicle Syndrome and Female Infertility

Tailai Chen,[1,2,3,7] Yuehong Bian,[1,2,3,7] Xiaoman Liu,[1,2,3] Shigang Zhao,[1,2,3] Keliang Wu,[1,2,3] Lei Yan,[1,2,3] Mei Li,[1,2,3] Zhenglin Yang,[6] Hongbin Liu,[1,2,3] Han Zhao,[1,2,3,*] and Zi-Jiang Chen[1,2,3,4,5,*]

Empty follicle syndrome (EFS) is defined as the failure to aspirate oocytes from mature ovarian follicles during in vitro fertilization. Except for some cases caused by pharmacological or iatrogenic problems, the etiology of EFS remains enigmatic. In the present study, we describe a large family with a dominant inheritance pattern of female infertility characterized by recurrent EFS. Genome-wide linkage analyses and whole-exome sequencing revealed a paternally transmitted heterozygous missense mutation of c.400 G>A (p.Ala134Thr) in zona pellucida glycoprotein 3 (*ZP3*). The same mutation was identified in an unrelated EFS pedigree. Haplotype analysis revealed that the disease allele of these two families came from different origins. Furthermore, in a cohort of 21 cases of EFS, two were also found to have the *ZP3* c.400 G>A mutation. Immunofluorescence and histological analysis indicated that the oocytes of the EFS female had degenerated and lacked the zona pellucida (ZP). ZP3 is a major component of the ZP filament. When mutant ZP3 was co-expressed with wild-type ZP3, the interaction between wild-type ZP3 and ZP2 was markedly decreased as a result of the binding of wild-type ZP3 and mutant ZP3, via dominant negative inhibition. As a result, the assembly of ZP was impeded and the communication between cumulus cells and the oocyte was prevented, resulting in oocyte degeneration. These results identified a genetic basis for EFS and oocyte degeneration and, moreover, might pave the way for genetic diagnosis of infertile females with this phenotype.

During in vitro fertilization (IVF) treatment, oocyte retrieval is performed after ovarian stimulation via vaginal puncture. Cumulus-oocyte complexes (COCs), which consist of cumulus cells surrounding the centrally located oocyte, are isolated from the individual's follicular fluid. As was first described by Coulam et al. in 1986, empty follicle syndrome (EFS) is a condition in which the ovarian response to stimulation and follicular development seems normal but no oocytes are retrieved for fertilization.[1] EFS can be classified as either false EFS (FEFS) or genuine EFS (GEFS). FEFS is mainly caused by pharmacological or iatrogenic problems; however, the etiology of GEFS, which is responsible for about 33% of EFS, still remains enigmatic.[2] It has been proposed that GEFS is caused by dysfunctional folliculogenesis, ovarian aging, or genetic factors including pericentric inversion of chromosome 2 and *LHCGR* (MIM: 152790) mutations.[3–7] A retrospective study of 12,359 individuals who underwent assisted reproductive technology (ART) revealed that the prevalence of GEFS was about 0.016%.[8] Without oocytes for fertilization, these individuals fail to achieve pregnancy after a demanding and expensive medical intervention, resulting in stress to both physicians and the individuals themselves.[9]

In this study, we identified a heterozygous missense mutation in *ZP3* (MIM: 182889; GenBank: NM_001110354.1) from a large family with multiple women affected by EFS. This mutation was also found in another family affected by EFS, as well as in two additional simplex cases with the same phenotype. In this study, we obtained donated in vitro matured oocytes for use as control oocytes and obtained control ovarian tissue from the ovarian wedge resection of an individual with polycystic ovary syndrome (PCOS). The institutional review board of the Center for Reproductive Medicine of Shandong University approved this study, and all participants provided written informed consent.

The proband of the family (Figure 1A, family A, III-10) was a 28-year-old woman with an 8-year history of primary infertility. She had normal ovarian reserves and regular menstrual cycles. Her basal sex hormone level was generally normal (Table S1), and other infertility-related assessments did not reveal any abnormalities. The couple had monitored ovulation in three natural cycles and subsequently underwent a cycle of clomiphene citrate combined with intrauterine insemination, but they failed to conceive. Given unexplained infertility, IVF treatment was offered. In the first attempt, a gonadotropin-releasing hormone (GnRH) agonist protocol was performed; the human chorionic gonadotropin (hCG) trigger was administered upon identification of 11 follicles measuring more than 14 mm in diameter and having a plasma estradiol level of 2,834 pg/mL. Oocyte retrieval was performed 36 hr after the hCG trigger, and 11 COCs were retrieved.

[1]Center for Reproductive Medicine, Shandong Provincial Hospital Affiliated to Shandong University, Jinan 250001, China; [2]National Research Center for Assisted Reproductive Technology and Reproductive Genetics, Jinan 250001, China; [3]The Key Laboratory for Reproductive Endocrinology, Shandong University, Ministry of Education, Jinan 250001, China; [4]Center for Reproductive Medicine, Ren Ji Hospital, School of Medicine, Shanghai Jiao Tong University, Shanghai 200135, China; [5]Shanghai Key Laboratory for Assisted Reproduction and Reproductive Genetics, Shanghai 200135, China; [6]The Key Laboratory for Human Disease Gene Study, Sichuan Academy of Medical Sciences and Sichuan Provincial People's Hospital, School of Medicine, University of Electronic Science and Technology of China, Chengdu 610072, China
[7]These authors contributed equally to this work
*Correspondence: hanzh80@yahoo.com (H.Z.), chenzijiang@hotmail.com (Z.-J.C.)
http://dx.doi.org/10.1016/j.ajhg.2017.08.001.

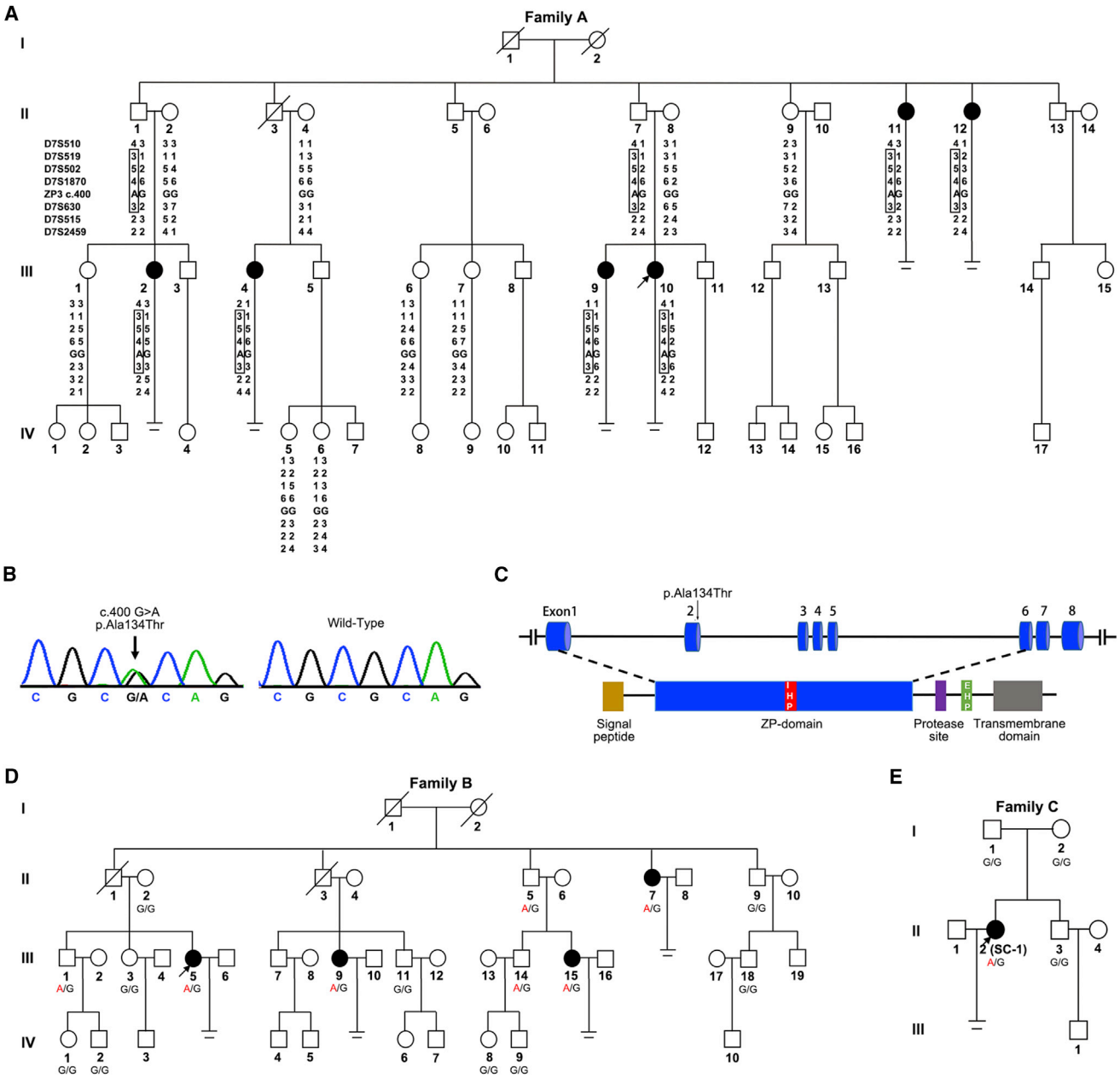

Figure 1. Pedigrees and Disease-Haplotype or Allele Segregation of Three Families Affected by Genuine Empty Follicle Syndrome
(A) Pedigree and disease-haplotype segregation of family A. Squares indicate male family members, and circles indicate female family members. Solid symbols represent affected subjects, and white indicates unaffected subjects; slashes represent deceased family members, and equal signs represent infertility. The arrow represents the proband of the family. The haplotypes for STR markers are shown in columns beneath family members who underwent linkage analysis. The disease-associated haplotypes are boxed.
(B) Sanger sequencing chromatograms of *ZP3* c.400 G>A (p.Ala134Thr) in affected and wild-type individuals.
(C) The schematic diagram of ZP3 with functional domains and the location of the identified variant. ZP3 peptide contains an N-terminal signal sequence (yellow), a ZP domain (blue) that consists of two subdomains (ZP-N and ZP-C), a C-terminal region that has a protease cleavage site (purple), an external hydrophobic patch (EHP, green), and a transmembrane domain (gray). An internal hydrophobic patch (IHP) is present in the short linker between ZP-N and ZP-C.
(D) Family B, with the mutation of *ZP3* c.400G>A (p.Ala134Thr). Genotypes are shown under each symbol.
(E) Family C, with the mutation of *ZP3* c.400G>A (p.Aala134Thr). Genotypes are shown under each symbol.

In contrast to control COCs, the cumulus cells of which were radiating and well expanded (Figure 2A, i), COCs from the proband had cumulus cells that were universally disorganized (Figure 2A, vi). In the 11 retrieved COCs, nine had no oocyte. After removal of the cumulus cells, the control oocyte exhibited a clear cytoplasm with homogeneous fine granularity and an intact ovoid first polar body (Figure 2A, ii), whereas in the two remaining COCs of the proband, the oocytes were degenerated (Figure 2A, vii). The second IVF attempt was performed 3 months later

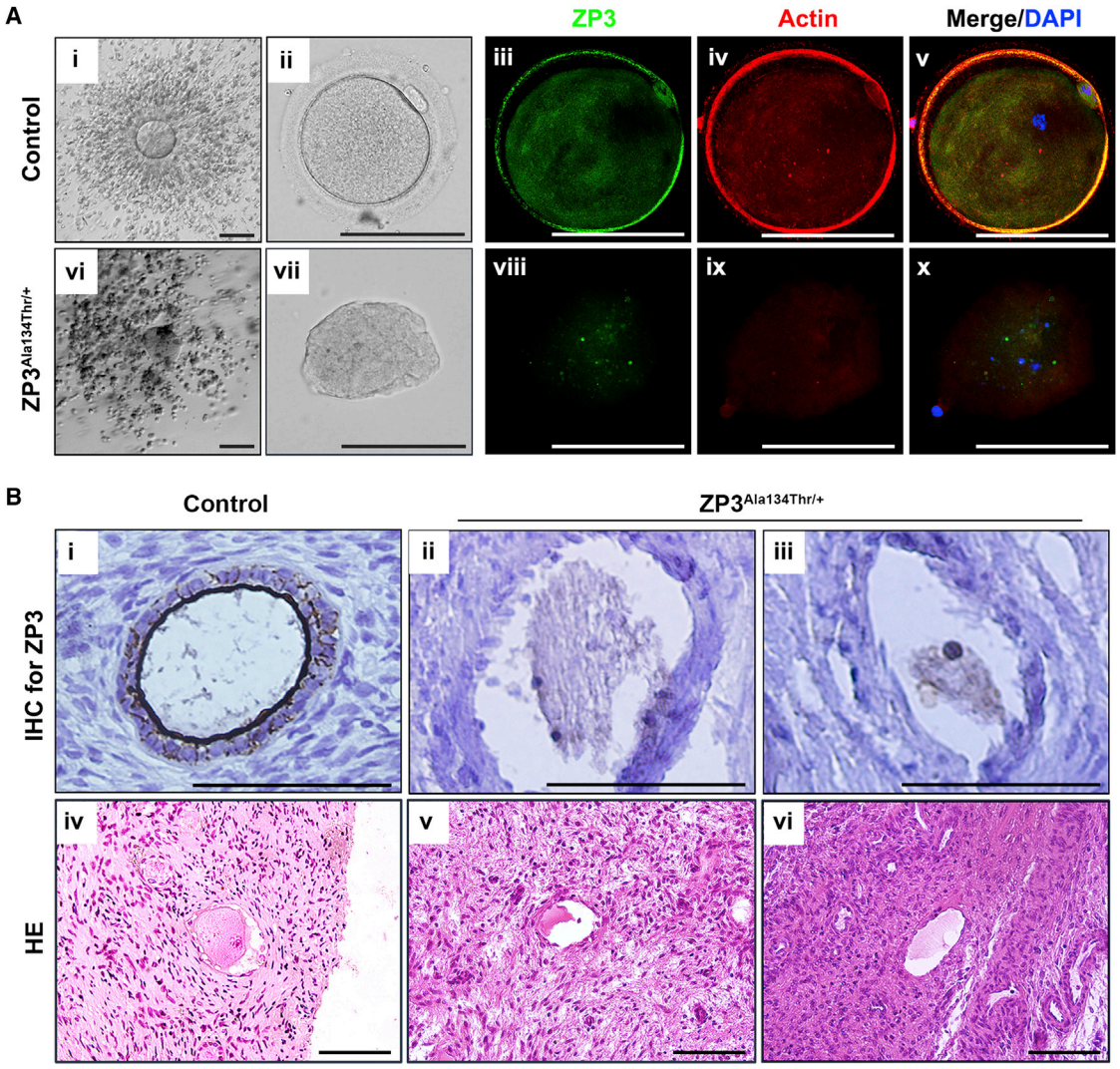

Figure 2. Pathological Changes of the Oocyte of Affected Individuals Harboring a *ZP3* Mutation
(A) The first column (i, vi) shows cumulus oocyte complexes of the control and the proband with ZP3 p.Ala134Thr. The second column shows oocytes removing cumulus cells. The right three columns (iii–v, viii–x) show oocytes imaged with confocal laser scanning microscopy. Fluorescent signals of ZP3 (green) and actin (red) were imaged individually. Nuclei were counterstained with DAPI (blue) and merged with ZP3 and actin images. Scale bar: 100 μm.
(B) Histologic findings of ovarian sections from the control and the proband with ZP3 p.Ala134Thr. The upper row shows immunohistochemical detection of ZP3 (brown staining), and the lower row shows the image of H&E staining. Scale bar: 100 μm.

according to a GnRH antagonist protocol; on trigger day, six follicles were greater than 14 mm in diameter, and estradiol level was 2,387 pg/mL. However, of the six retrieved COCs, four were empty and two were found to contain degenerated oocytes lacking zonae pellucidae (ZP). In the third attempt, HMG was administered; the estradiol level reached 2,358 pg/mL, and seven follicles were larger than 14 mm on trigger day. Seven COCs were retrieved, but all were empty, and only small fragments of ooplasm could be seen. The sister (family A, III-9) of the index case followed a similar course in her three IVF cycles. At each egg retrieval, most of the cumulus complexes were empty and had no oocytes; only a few contained degenerated oocytes, which had no ZP (Table S1). Two paternal aunts and two cousins of the proband also suffered unexplained primary infertility. As shown in the family pedigree, the disorder appeared to be segregating in an autosomal-dominant, female-limited fashion.

We collected blood samples from 23 members of family A. Genomic DNA was extracted by QIAamp DNA blood mini kit (QIAGEN) according to the manufacturer's instructions. In order to identify disease-associated regions, we performed a genome-wide linkage scan on 17 family members. Three hundred sixty-six short tandem repeat (STR) markers with an average spacing of about 10 cM were genotyped and logarithm of odds (LOD) scores were calculated assuming a model of an autosomal dominant disease with complete penetrance using MERLIN software. The genome-wide linkage analysis yielded a maximum LOD score of 2.35 in chromosome 7, and the common minimal region was chromosome 7p12.3–q21.13 (Figure 1A).

To determine the causative mutation, we carried out whole-exome sequencing (WES). Because we predicted that the mutation would be paternally transmitted in an autosomal-dominant manner, we selected three affected females (family A, II-11, III-2 and III-10) and two potential male carriers (II-1, II-7) as well as two unaffected females (II-2, II-8) for WES. Agilent SureSelect Human All Exon V4+UTR kit was used for library preparation, and sequencing was performed on an Illumina HiSeq 2000 platform. Sequencing reads were aligned to the human genome (hg19), and a variant was selected as a potential candidate for the phenotype if it met the following conditions: (1) it was present in all three affected females and two male carriers, (2) it was absent in the two unaffected females, and (3) it had not previously been reported or had been reported to have a frequency below 1% in public databases, including dbSNP, 1000 Genomes Browser, the NHLBI Exome Variant Server (EVS), and the Exome Aggregation Consortium (ExAC) Browser. Subsequently, Sanger sequencing was carried out for the selected variants in 16 additional family members. This strategy revealed a heterozygous missense variant, c.400G>A (p.Ala134Thr), in exon 2 of *ZP3* (GenBank: NM_001110354.1), as the potential pathogenic variant (Figures 1B and 1C), segregating perfectly with the disease status in affected and unaffected female individuals of the family (Figure S1A). This mutation was also absent in our in-house 2,213 population-based Han Chinese controls and 400 healthy Han Chinese women with normal fertility. Moreover, it was absent from the gnomAD database. It is noteworthy that this variant was found on chromosome 7q11.23, which localized to our previously identified disease-associated region by linkage analysis. Thus, *ZP3* c.400G>A (p.Ala134Thr) is the mutation responsible for the phenotype of EFS in this family.

To further investigate the relationship between *ZP3* c.400G>A and EFS, we analyzed another family (Figure 1D, family B) exhibiting the same phenotype (Table S1). Sanger sequencing of *ZP3* was performed on 16 members of family B, and c.400G>A was found to co-segregate with disease status in this family as well (Figure 1D). Furthermore, four STR markers located near the mutation (two markers upstream and two markers downstream) were genotyped. Haplotype analysis revealed that the disease allele origins of family A and family B were independent (Figures S1A and S1B). In addition, a cohort of 21 individuals who exhibited EFS during IVF attempts were recruited and sequenced for *ZP3*. The same heterozygous mutation of c.400G>A was identified in two individuals (SC-1 and SC-2 in Table S1), who were both simplex cases. The parents of SC-1 were both wild-type at this allele, suggesting the mutation of SC-1 was de novo (Figure 1E, family C), whereas no DNA was available from the parents of SC-2. Taken together, these results lead us to conclude that *ZP3* c.400G>A (p.Ala134Thr) is the mutation responsible for EFS.

ZP3 encodes the ZP3 glycoprotein, which is a component of human ZP.[10] ZP3 is expressed specifically in oocytes, which explains why the phenotype was limited to females. The ZP is a thick extracellular coat that surrounds mammalian oocytes.[11] Its functions include recognizing gametes, supporting oocyte-follicle cell communication, and protecting the oocyte.[12–14] To explore the relationship between ZP3 and EFS, we first conducted immunofluorescence analysis of ZP3 localization in the degenerated oocytes of the proband of family A (III-10). Oocytes of the proband and normal control were labeled with anti-ZP3 (Proteintech) and anti-actin (Sigma-Aldrich) antibodies. The nucleus was counterstained with 4′,6′-diamidino-2-phenylindole (DAPI). The stained specimens were examined with a confocal laser-scanning microscope. In the control oocyte, ZP3 signals were concentrated in the surrounding ZP and were also detected diffusely in the ooplasm (Figure 2A, iii–v); however, ZP3 was barely detectable in the proband's oocyte (Figure 2A, viii–x). In addition, the nucleus was totally disassembled (Figure 2A, x), which further confirmed degeneration of the oocyte. Subsequently, to detect the morphology of the proband's follicle before ovulation, we performed histological analysis of the ovary. Ovarian cortical biopsy was conducted on the proband of family A (III-10) by laparoscopy; tissue from ovarian wedge resection of a PCOS individual whose oocyte morphology was normal served as the control. H&E stain and ZP3 immunohistochemistry (IHC) staining were conducted in ovarian sections. In the control ovary, contrast staining revealed a distinct outline of the ZP surrounding the oocyte (Figure 2B, i, iv), whereas the proband's oocyte had neither an obvious ZP3 signal nor a ZP (Figure 2B, ii, iii, v, vi). Additionally, morphological abnormalities of the oocyte could be observed in preantral follicles from the same person. These results showed that the oocytes of the proband degenerated before ovulation in the absence of a ZP. We concluded that the oocytes of the proband were totally degenerated or collapsed and that this is why COCs were empty upon retrieval.

In human ZP assembly, ZP2, ZP3, and ZP4 form long filaments cross-linked by ZP1.[15,16] The p.Ala134Thr substitution affects the ZP domain of ZP3 (Figure 1C), which is characterized by the presence of eight conserved cysteine residues and is important for protein-protein interactions.[17,18] The amino acid substitution caused by the mutation resulted in conversion of an alanine residue to a threonine. This alanine residue was conserved among the vast majority of species, from zebrafish to macaques and humans, but not in rodents such as mice and rats, which have a valine residue at this site (Figure S2). The alteration in rodents is unlikely to be significant because valine is quite similar to alanine; both residues are nonpolar, aliphatic, and hydrophobic, whereas the mutated threonine residue is polar, uncharged, and hydrophilic. Functional prediction by PyMOL software showed that the mutation could alter the structure of ZP3 (Figure 3A). To elucidate the molecular mechanism of how p.Ala134Thr led to ZP absence and oocyte degeneration, we constructed

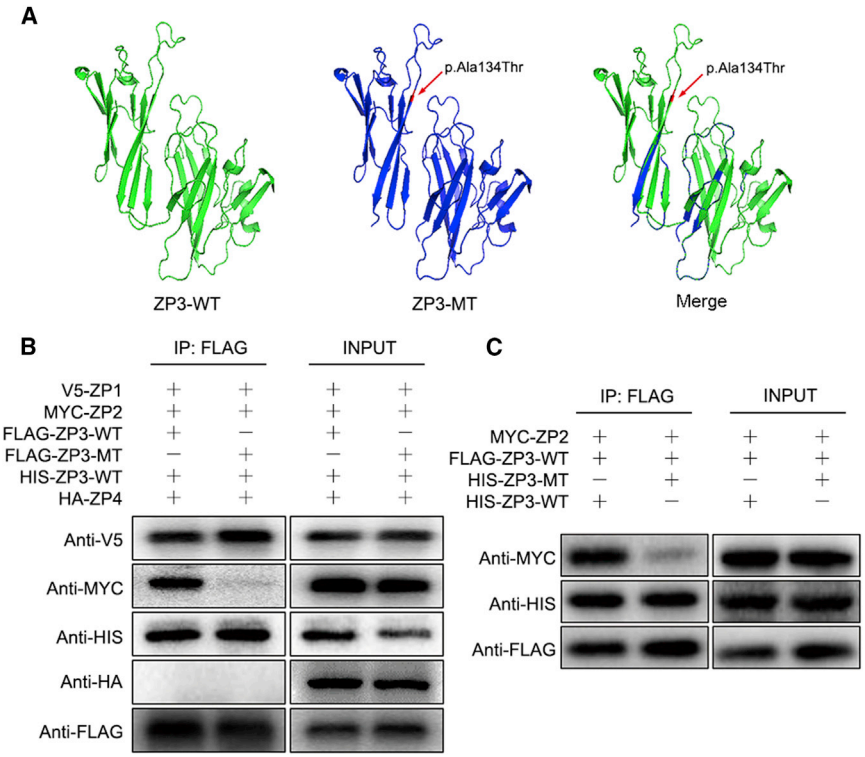

Figure 3. Functional Study of c.400 G>A in *ZP3*

(A) The structure prediction of wild-type (left) and mutant (middle) ZP3 and a merged image (right) created by PyMOL software. The mutation (c.400G>A [p.Ala134Thr], red arrow) leads to protein structure changes.

(B) The interactions of $ZP3^{WT}$ and $ZP3^{MT}$ with ZP glycoproteins. Lanes 1 and 3 show FLAG-$ZP3^{WT}$ co-transfected with V5-ZP1, MYC-ZP2, HIS-$ZP3^{WT}$, and HA-ZP4; lane 1 shows co-immunoprecipitation by anti-FLAG antibody, and lane 3 shows input. Lanes 2 and 4 show FLAG-$ZP3^{MT}$ co-transfected with V5-ZP1, MYC-ZP2, HIS-$ZP3^{WT}$, and HA-ZP4; lane 2 shows co-immunoprecipitation by anti-FLAG antibody, and lane 4 shows input.

(C) The dominant-negative effect of the ZP3 p.Ala134Thr variant. Lanes 1 and 3 show FLAG-$ZP3^{WT}$ co-transfected with MYC-ZP2 and HIS-$ZP3^{WT}$, lane 1 shows co-immunoprecipitation by anti-FLAG antibody and lane 3 shows input. Lanes 2 and 4 show HIS-$ZP3^{MT}$ co-transfected with MYC-ZP2 and FLAG-$ZP3^{WT}$; lane 2 shows co-immunoprecipitation by anti-FLAG antibody, and lane 4 shows input.

expression vectors for FLAG-$ZP3^{WT}$ (FLAG-tagged wild-type human ZP3), FLAG-$ZP3^{MT}$ (FLAG-tagged human mutant ZP3 with p.Ala134Thr), HIS-$ZP3^{WT}$ (HIS-tagged wild-type human ZP3), HIS-$ZP3^{MT}$ (HIS-tagged human mutant ZP3 with p.Ala134Thr), V5-ZP1 (V5-tagged human ZP1), MYC-ZP2 (MYC-tagged human ZP2), and HA-ZP4 (HA-tagged human ZP4) by cloning the coding region into the pcDNA3.1 plasmid. We then transfected expression vectors into CHO-K1 cells and performed co-immunoprecipitation (Co-IP) analysis to explore interactions between ZP3 and other ZP glycoproteins. We extracted protein from transfected cells by targeting the anti-FLAG antibody (Abcam), then performed immuloblotting to detect co-precipitated ZP glycoproteins. When FLAG-$ZP3^{WT}$ was co-transfected with V5-ZP1, MYC-ZP2, HIS-$ZP3^{WT}$, and HA-ZP4, $ZP3^{WT}$ interacted with ZP1, ZP2, and $ZP3^{WT}$ but did not interact with ZP4 (Figure 3B). When FLAG-$ZP3^{MT}$ was co-transfected with V5-ZP1, MYC-ZP2, HIS-$ZP3^{WT}$, and HA-ZP4, unlike $ZP3^{WT}$, $ZP3^{MT}$ had no interaction with ZP2 (Figure 3B). Next, HIS-$ZP3^{WT}$ or HIS-$ZP3^{MT}$ was co-transfected with FLAG-$ZP3^{WT}$ or MYC-ZP2, respectively. As a result, despite the fact that $ZP3^{WT}$ could bind with ZP2, the interaction between $ZP3^{WT}$ and ZP2 was largely diminished when $ZP3^{MT}$ was also present (Figure 3C). In addition, binding between $ZP3^{WT}$ and $ZP3^{MT}$ was observed and might affect the interaction between $ZP3^{WT}$ and ZP2. These results indicate that the ZP3 substitution p.Ala134Thr has a dominant-negative effect that influences the binding between $ZP3^{WT}$ and ZP2. The interruption of the binding between $ZP3^{WT}$ and ZP2 probably impedes ZP assembly. By extending processes that traverse the ZP, the innermost layer of cumulus cells establishes strong connections with the oocyte.[19] When the ZP is absent, the communication pathway between cumulus cells and the oocyte might be interrupted, thereby resulting in degeneration of the oocyte.

In previous genetic studies of EFS, two different homozygous missense mutations in luteinizing hormone/choriogonadotropin receptor (*LHCGR*) were identified from two pedigrees.[6,7] The administration of β-HCG elicited no response in individuals with these mutations, thus resulting in EFS. In these two pedigrees, neither oocytes nor COCs were recovered from the probands. However, in our study we describe a different condition whereby COCs could be detected, but the oocytes were completely degenerated inside the COCs.

Previously, Huang et al. identified a homozygous frameshift mutation of *ZP1* (MIM: 195000) inherited in recessive fashion from a family exhibiting oocytes devoid of a ZP.[20] The frameshift mutation formed a premature stop codon and resulted in a truncated ZP1, which was postulated to sequester ZP3 in the cytoplasm and prevent the formation of a ZP by working in loss-of-function way. In our study, the heterozygous p.Ala134Thr substitution in ZP3 impeded the interaction between ZP3 and ZP2 and eventually led to oocyte degeneration, by working in a dominant-negative way. It has been demonstrated that female *Zp3*-deficient mice are completely infertile. Even though COCs could be retrieved in the oviducts after superovulation, few or no oocytes could be found, and any oocytes recovered from COCs lacked a ZP,[21,22] which is consistent with the clinical manifestation of the individuals carrying

the *ZP3* c.400 G>A (p.Ala134Thr) mutation in the present study.

Recently, Gao et al. reported a role for *ZP3* in germinal vesicle breakdown (GVBD).[23] They knocked down ZP3 in mouse oocytes in vitro by siRNA transfection and found that GVBD was dramatically inhibited. The p.Ala134Thr variant we identified mainly resulted in oocyte degeneration and EFS, which could occur even before GVBD. Thus, whether this mutation could inhibit GVBD requires further investigation.

In conclusion, we have identified a *ZP3* mutation, c.400 G>A (p.Ala134Thr), responsible for EFS. The mutation could destroy the assembly of the ZP and lead to oocyte degeneration, resulting in empty COCs. Our study provides evidence for a genetic basis of EFS as well as support for the genetic diagnosis of infertile individuals with this phenotype.

Accession Numbers

The accession number for the *ZP3* variant c.400 G>A (p.Ala134Thr) reported in this paper is ClinVar: SCV000584171.

Supplemental Data

Supplemental Data include two figures and one table and can be found with this article online at http://dx.doi.org/10.1016/j.ajhg.2017.08.001.

Acknowledgments

This research was supported by the National Key Research and Development Program of China (2017YFC1001500, 2017YFC1001000, 2016YFC1000600), the National Natural Science Foundation of China (31371453, 31571548, 81622021, 81430029, 81601256, 81401266, 81490743), and the Young Scholars Program of Shandong University (2015WLJH54). The authors thank all participants. We thank Prof. Xue Zhang at Peking Union Medical College, China for his kind suggestions in Co-IP experiment and manuscript preparation. We are grateful to Prof. Qiji Liu at Shandong University, China for suggestions on linkage analyses; to Dr. Lulin Huang at the Key Laboratory for Human Disease Gene Study at the Sichuan Academy of Medical Sciences for sharing the exome sequencing data of 2213 population controls; and to Bin Wu from Guangdong Provincial Hospital for Traditional Chinese Medicine for bioinformatic analysis. We also thank Dr. Antoni Duleba from UCSD School of Medicine, USA for revising the manuscript.

Received: March 28, 2017
Accepted: July 31, 2017
Published: August 31, 2017

Web Resources

1000 Genomes, http://www.1000genomes.org
ClinVar, https://www.ncbi.nlm.nih.gov/clinvar/
dbSNP, http://www.ncbi.nlm.nih.gov/projects/SNP/
ExAC Browser, http://exac.broadinstitute.org/
GenBank, http://www.ncbi.nlm.nih.gov/genbank/
GnomAD database, http://gnomad.broadinstitute.org/
NHLBI Exome Sequencing Project (ESP) Exome Variant Server, http://evs.gs.washington.edu/EVS/
OMIM, http://www.omim.org/

References

1. Coulam, C.B., Bustillo, M., and Schulman, J.D. (1986). Empty follicle syndrome. Fertil. Steril. *46*, 1153–1155.
2. Stevenson, T.L., and Lashen, H. (2008). Empty follicle syndrome: the reality of a controversial syndrome, a systematic review. Fertil. Steril. *90*, 691–698.
3. Awonuga, A., Govindbhai, J., Zierke, S., and Schnauffer, K. (1998). Continuing the debate on empty follicle syndrome: can it be associated with normal bioavailability of beta-human chorionic gonadotrophin on the day of oocyte recovery? Hum. Reprod. *13*, 1281–1284.
4. Lorusso, F., Depalo, R., Tsadilas, S., Caradonna, F., Di Gilio, A., Capotorto, M.T., Vacca, M., Nappi, L., and Selvaggi, L. (2005). Is the occurrence of the empty follicle syndrome a predictor that a subsequent stimulated cycle will be an unfavourable one? Reprod. Biomed. Online *10*, 571–574.
5. Vujisic, S., Stipoljev, F., Bauman, R., Dmitrovic, R., and Jezek, D. (2005). Pericentric inversion of chromosome 2 in a patient with the empty follicle syndrome: case report. Hum. Reprod. *20*, 2552–2555.
6. Yariz, K.O., Walsh, T., Uzak, A., Spiliopoulos, M., Duman, D., Onalan, G., King, M.-C., and Tekin, M. (2011). Inherited mutation of the luteinizing hormone/choriogonadotropin receptor (LHCGR) in empty follicle syndrome. Fertil. Steril. *96*, e125–e130.
7. Yuan, P., He, Z., Zheng, L., Wang, W., Li, Y., Zhao, H., Zhang, V.W., Zhang, Q., and Yang, D. (2017). Genetic evidence of 'genuine' empty follicle syndrome: a novel effective mutation in the LHCGR gene and review of the literature. Hum. Reprod. *32*, 944–953.
8. Mesen, T.B., Yu, B., Richter, K.S., Widra, E., DeCherney, A.H., and Segars, J.H. (2011). The prevalence of genuine empty follicle syndrome. Fertil. Steril. *96*, 1375–1377.
9. Zreik, T.G., Garcia-Velasco, J.A., Vergara, T.M., Arici, A., Olive, D., and Jones, E.E. (2000). Empty follicle syndrome: evidence for recurrence. Hum. Reprod. *15*, 999–1002.
10. Lefièvre, L., Conner, S.J., Salpekar, A., Olufowobi, O., Ashton, P., Pavlovic, B., Lenton, W., Afnan, M., Brewis, I.A., Monk, M., et al. (2004). Four zona pellucida glycoproteins are expressed in the human. Hum. Reprod. *19*, 1580–1586.
11. Wassarman, P.M. (2008). Zona pellucida glycoproteins. J. Biol. Chem. *283*, 24285–24289.
12. Wassarman, P.M., Jovine, L., and Litscher, E.S. (2001). A profile of fertilization in mammals. Nat. Cell Biol. *3*, E59–E64.
13. Matzuk, M.M., Burns, K.H., Viveiros, M.M., and Eppig, J.J. (2002). Intercellular communication in the mammalian ovary: oocytes carry the conversation. Science *296*, 2178–2180.
14. Conner, S.J., Lefièvre, L., Hughes, D.C., and Barratt, C.L. (2005). Cracking the egg: increased complexity in the zona pellucida. Hum. Reprod. *20*, 1148–1152.
15. Green, D.P. (1997). Three-dimensional structure of the zona pellucida. Rev. Reprod. *2*, 147–156.
16. Monné, M., and Jovine, L. (2011). A structural view of egg coat architecture and function in fertilization. Biol. Reprod. *85*, 661–669.

17. Monné, M., Han, L., Schwend, T., Burendahl, S., and Jovine, L. (2008). Crystal structure of the ZP-N domain of ZP3 reveals the core fold of animal egg coats. Nature *456*, 653–657.
18. Han, L., Monné, M., Okumura, H., Schwend, T., Cherry, A.L., Flot, D., Matsuda, T., and Jovine, L. (2010). Insights into egg coat assembly and egg-sperm interaction from the X-ray structure of full-length ZP3. Cell *143*, 404–415.
19. Gilula, N.B., Epstein, M.L., and Beers, W.H. (1978). Cell-to-cell communication and ovulation. A study of the cumulus-oocyte complex. J. Cell Biol. *78*, 58–75.
20. Huang, H.L., Lv, C., Zhao, Y.C., Li, W., He, X.M., Li, P., Sha, A.G., Tian, X., Papasian, C.J., Deng, H.W., et al. (2014). Mutant ZP1 in familial infertility. N. Engl. J. Med. *370*, 1220–1226.
21. Liu, C., Litscher, E.S., Mortillo, S., Sakai, Y., Kinloch, R.A., Stewart, C.L., and Wassarman, P.M. (1996). Targeted disruption of the mZP3 gene results in production of eggs lacking a zona pellucida and infertility in female mice. Proc. Natl. Acad. Sci. USA *93*, 5431–5436.
22. Rankin, T., Familari, M., Lee, E., Ginsberg, A., Dwyer, N., Blanchette-Mackie, J., Drago, J., Westphal, H., and Dean, J. (1996). Mice homozygous for an insertional mutation in the Zp3 gene lack a zona pellucida and are infertile. Development *122*, 2903–2910.
23. Gao, L.L., Zhou, C.X., Zhang, X.L., Liu, P., Jin, Z., Zhu, G.Y., Ma, Y., Li, J., Yang, Z.X., and Zhang, D. (2017). ZP3 is Required for Germinal Vesicle Breakdown in Mouse Oocyte Meiosis. Sci. Rep. *7*, 41272.